Article

Co(III)-NTA mediated antigen immobilization on a fiber optic-SPR biosensor for detection of autoantibodies in autoimmune diseases: application in immune-mediated thrombotic thrombocytopenic purpura

Sara Horta, Jia-Huan Qu, Charlotte Dekimpe, Quintijn Bonnez, Aline Vandenbulcke, Edwige Tellier, Gilles Kaplanski, Filip Delport, Nick Geukens, Jeroen Lammertyn, and Karen Vanhoorelbeke

Anal. Chem., **Just Accepted Manuscript** • DOI: 10.1021/acs.analchem.0c02586 • Publication Date (Web): 15 Sep 2020

Co(III)-NTA mediated antigen immobilization on a fiber optic-SPR biosensor for detection of autoantibodies in autoimmune diseases: application in immune-mediated thrombotic thrombocytopenic purpura

Sara Horta[1,2], Jia-Huan Qu[2], Charlotte Dekimpe[1], Quintijn Bonnez[1], Aline Vandenbulcke[1], Edwige Tellier[3], Gilles Kaplanski[3,4], Filip Delport[5], Nick Geukens[6], Jeroen Lammertyn[2,*], Karen Vanhoorelbeke[1,6,*]

[1]Laboratory for Thrombosis Research, IRF Life Sciences, KU Leuven Campus Kulak Kortrijk, Etienne Sabbelaan 53 8500 Kortrijk, Belgium
[2]Department of Biosystems, Biosensors Group, KU Leuven, Willem De Croylaan 42 B-3001 Heverlee, Belgium
[3]Aix Marseille Univ, INSERM, INRAE, C2VN, Jardin du Pharo, 58 Boulevard Charles Livon, 13007 Marseille, France
[4]Aix Marseille Univ, APHM, INSERM, INRAE, C2VN, Hôpital de la Conception, Service de médecine interne, 147 Boulevard Baille, 13005, Marseille, France
[5]FOx Biosystems NV, Bioville, Agoralaan Abis, 3590 Diepenbeek, Belgium
[6]PharmAbs, The KU Leuven Antibody Center, KU Leuven, Herestraat 49, 3000 Leuven, Belgium
*Last authors and corresponding authors. Email: Jeroen.Lammertyn@kuleuven.be and Karen.Vanhoorelbeke@kuleuven.be

ABSTRACT: Autoantibodies are key biomarkers in clinical diagnosis of autoimmune diseases routinely detected by enzyme-linked immunosorbent assays (ELISA). However, the complexity of these assays is limiting their use in routine diagnostics. Fiber optic-surface plasmon resonance (FO-SPR) can overcome these limitations but improved surface chemistries are still needed to guarantee detection of autoantibodies in complex matrices. In this paper we describe the development of an FO-SPR immunoassay for the detection of autoantibodies in plasma samples from immune-mediated thrombotic thrombocytopenic purpura (iTTP) patients. Hereto hexahistidine tagged recombinant ADAMTS13 (rADAMTS13-His_6) was immobilized on nitrilotriacetic acid (NTA)-coated FO probes chelated by cobalt (Co(III)) and exposed to anti-ADAMTS13 autoantibodies. Initial studies were performed to optimize rADAMTS13-His_6 immobilization and to confirm the specificity of the immunoassay for detection of anti-ADAMTS13 autoantibodies with FO-SPR. The performance of the immunoassay was then evaluated by comparing Co(III)- and nickel (Ni(II))-NTA stabilized surfaces, confirming the stable immobilization of the antigen in Co(III)-NTA functionalized FO probes. A calibration curve was prepared with a dilution series of a cloned human anti-ADAMTS13 autoantibody in ADAMTS13-depleted plasma resulting in an average inter-assay coefficient of variation of 7.1 % and a limit of detection of 0.24 ng/mL. Finally, the FO-SPR immunoassay was validated using seven iTTP patient plasma samples resulting in an excellent correlation with an in-house developed ELISA (r = 0.973). In summary, the specificity and high sensitivity in combination with a short time-to-result (2.5h compared to 4-5h for a regular ELISA) makes the FO-SPR immunoassay a powerful assay for routine diagnosis of iTTP and with extension for any other autoimmune disease.

Autoimmune diseases occur when the immune system loses tolerance to certain self-antigens and generates autoantibodies against these self-antigens[1,2]. Up to 100 types of different autoimmune disorders have been described and their frequency has significantly increased over the last 30 years with a current incidence of 5-10 % worldwide[2,3]. Immune-mediated thrombotic thrombocytopenic purpura (iTTP) is a rare thrombotic microangiopathy caused by the presence of autoantibodies against the von Willebrand factor (VWF) cleaving protease ADAMTS13 (A Disintegrin And Metalloprotease with ThromboSpondin type 1 repeats, member 13)[4–6]. In healthy individuals, ADAMTS13 cleaves ultra-large prothrombotic VWF multimers into smaller less active proteins. In iTTP patients, anti-ADAMTS13 autoantibodies either inhibit or clear ADAMTS13, resulting in the accumulation of prothrombotic VWF multimers, which spontaneously bind platelets leading to the formation of microthrombi in capillaries and/or arterioles in different organs. Organs are deprived of nutrients and oxygen, leading to the death of patients when left untreated. The measurement of anti-ADAMTS13 autoantibodies levels in circulation is therefore crucial for the diagnosis, treatment and prognosis of the disease[4,7]. Conventional enzyme-linked immunosorbent assay (ELISA)s are the gold standard for the detection of anti-ADAMTS13 autoantibodies in iTTP patients[4,8,9], however, this type of assay is complex and has a long turn-over time limiting its use in routine diagnostics.

Biosensors are analytical devices that can detect a molecule of interest by generating a measurable signal upon the specific interaction of this target molecule with a biorecognition

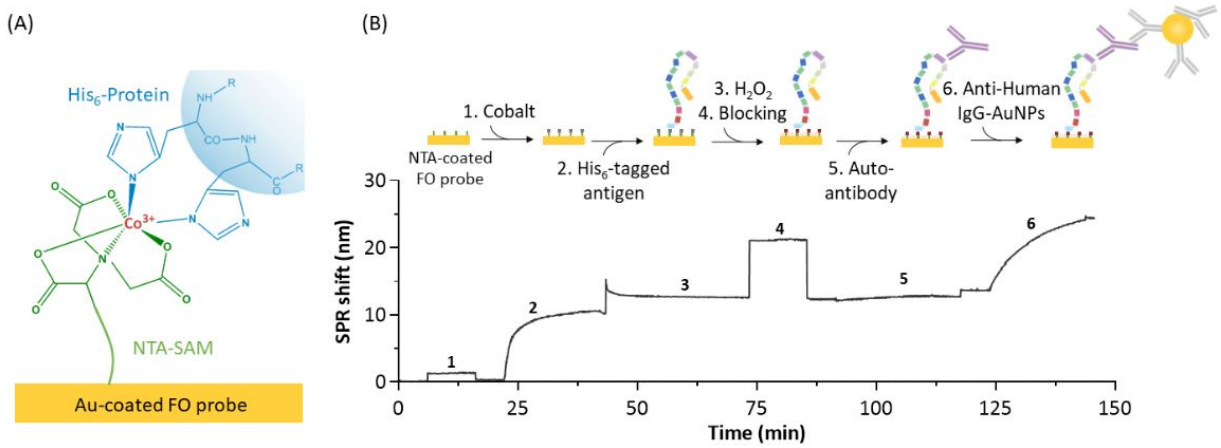

Figure 1. Schematic representation of FO-SPR immunoassay for the detection of anti-ADAMTS13 autoantibodies. A) Interaction of a His_6-tagged protein to NTA-Co(III). B) Sensorgram of the FO-SPR immunoassay for detection of anti-ADAMTS13 autoantibodies in an NTA-Co(III)-rADAMTS13-His_6 coated FO probe.

element[10]. Among the different biosensing technologies, fiber optic-surface plasmon resonance (FO-SPR) is a fully automated platform based on measuring the refractive index shift that occurs in response to the molecular interaction between the analyte and the metal surface-bound bioreceptor[11]. The sensing component corresponds to an inexpensive and disposable FO probe that can be simply dipped in the analyte solution, allowing execution of sensitive and reproducible assays in short period of time. This technology has been so far described for the detection of anti-drug antibodies[12–14] and fibrinogen[15] in patient samples.

Detection of autoantibodies in patient plasma or serum requires the coupling of the recombinant antigen of interest to the FO-SPR biosensor surface. Depending on the autoimmune disease, the antigen of interest can be i.e. an antibody, protease, glycoprotein or citrullinated peptide. The immobilization of the antigen is mostly done by covalent amine coupling between amino groups of the recombinant antigen and the activated carboxylic linkers on the FO-SPR biosensor surface[13]. However, despite the simplicity of this method, the covalent amino coupling leads to random orientation of the immobilized antigen[16] and can lead to conformational changes in the antigen, resulting in the loss of binding of some autoantibodies. These drawbacks can be solved by using a recombinant antigen with an affinity tag such as a hexahistidine (His_6)-tag, that allows the oriented immobilization of the antigen on nitrilotriacetic acid (NTA)-functionalized surfaces via histidine chelation with bivalent cations like nickel (Ni(II)) or cobalt (Co(II))[17–19]. An additional advantage of this immobilization strategy is that it can be used for autoantibody detection against any self-antigen (in any autoimmune disease), provided the self-antigen is available as a recombinant protein with a His_6-tag. However the low binding affinity between the NTA-Ni(II) or NTA-Co(II) and the His_6-tagged protein makes this approach sensitive to antigen exchange when using biological samples like plasma or serum (as metal-binding proteins are found in human plasma) or when using chelators as ethylenediaminetetraacetic acid (EDTA)[18,20,21].

Several strategies have been described to improve the affinity between the NTA and the His_6-tagged recombinant proteins in the context of biosensing[21,22]. Wegner et al. (2013) described a stable immobilization of His_6-tagged proteins to NTA by oxidizing the chelating metal cobalt, Co(II), to Co(III). This step reduces the dissociation constant of the NTA-Co(III)-His_6-tagged protein thereby generating a more stable complex[23,24]. This approach was validated using a quartz crystal microbalance with dissipation (QCM-D)[24] and biolayer interferometry (BLI)[25]. In our recently published report, we described for the application of Co(III)-NTA chemistry in FO-SPR biosensors[26]. However, this strategy was never characterized with clinical samples neither implemented for detection of autoantibodies for diagnostic purposes.

In the current study, we present for the first time the development of an FO-SPR autoantibody assay for efficient, simple and fast detection of autoantibodies in plasma of patients suffering from the autoimmune disease iTTP. Hereto, recombinant His_6-tagged ADAMTS13 (rADAMTS13-His_6) is immobilized on the NTA-Co(III) activated FO-SPR biosensor. To develop the autoantibody assay, several steps are studied: (i) the optimal antigen concentration and buffer for antigen immobilization on the FO-SPR biosensor, (ii) the sensitivity and specificity of the immunoassay and (iii) the performance of the NTA-Co(III)-rADAMTS13-His_6 complex compared to the NTA-Ni(II)-rADAMTS13-His_6 complex for the detection of anti-ADAMTS13 autoantibodies in both buffer and plasma samples. A calibration curve in diluted plasma is further built to evaluate the analytical performance of the biosensor for detecting anti-ADAMTS13 autoantibodies. Finally, anti-ADAMTS13 autoantibody titers are determined in seven iTTP plasma samples using the FO-SPR immunoassay and compared to the titers determined in the in-house developed anti-ADAMTS13 autoantibody ELISA.

With this study, we are aiming to develop a fast and easy-to-use FO-SPR assay for the diagnosis of iTTP in healthcare centers. The applicability of the current FO-SPR platform is large, as it can be developed for any autoimmune disease where a His_6-tagged antigen is available, and autoantibodies need to be detected.

EXPERIMENTAL SECTION

Materials and reagents. His_6-tagged recombinant ADAMTS13 (rADAMTS13-His_6) was produced, purified and quantified in-house as previously described[27]. The human monoclonal anti-ADAMTS13 autoantibody II-1 is a recombinant autoantibody cloned from an iTTP patient that recognizes the spacer domain of human ADAMTS13[28]. The

mouse monoclonal anti-human ADAMTS13 antibody 17C7 is an in-house developed antibody that recognizes the metalloprotease domain of human ADAMTS13[29]. NTA-terminated self-assembled monolayers (SAMs) formation reagent was obtained from Dojindo Laboratories (Kumamoto, Japan). 4-(2-hydroxyethyl)-1-piperazineethanesulfonic acid (HEPES, > 99.5 %), hydrogen peroxide solution (H_2O_2, 30 %), bovine serum albumin (BSA, ≥ 98 %), Sodium phosphate dibasic dihydrate ($Na_2HPO_4.2H_2O$, ≥ 99 %), o-phenylenediamine (OPD) and rabbit anti-goat immunoglobulin G (IgG) labelled with horseradish peroxidase (HRP) were purchased from Sigma-Aldrich (Bornem, Belgium). Ethanol (C_2H_5OH, 99.8 %), cobalt(II) chloride hexahydrate ($CoCl_2 \cdot 6H_2O$), nickel(II) sulfate hexahydrate ($NiSO_4 \cdot 6H_2O$), potassium chloride (KCl, 99 %) and monopotassium phosphate (KH_2PO_4, 99 %) were purchased from Acros Organics (Geel, Belgium). Sodium carbonate (Na_2CO_3) was purchased from Chemlab (Zedelgem, Belgium) and Trident 1 M Tris-HCl was supplied by Bio-Connect (Huissen, the Netherlands). Tween 20 was purchased from AppliChem GmbH (Darmstadt, Germany) and powdered milk was purchased in Carl Roth (Karlsruhe, Germany). Sodium chloride (NaCl), Dynabeads™ M-280 tosylactivated, SuperBlock™ (TBS) blocking buffer, Pierce™ nickel-coated plates (clear, 96-well), goat anti-human IgG antibodies, human IgG Isotype control (non-specific IgG) and tetramethylbenzidine (TMB) Substrate Solution were purchased from Thermo Fisher Scientific (Merelbeke, Belgium). Gold nanoparticles (AuNPs) with a diameter of 20 nm were purchased by BBI solutions (Cardiff, UK). Buffers were prepared as follows: HEPES buffer (10 mM HEPES at pH 7.4), phosphate buffered saline (PBS) (13.7 mM NaCl, 0.27 mM KCl, 0.65 mM $Na_2HPO_4.2H_2O$ and 0.15 mM KH_2PO_4 at pH 7.4) and Tris-NaCl buffer (50 mM Tris-HCl and 300 mM NaCl at pH 7.4). All buffers were prepared with deionized water purified by a Milli-Q plus system (MQ water) (Millipore, Marlborough, USA).

Plasma samples. Citrated plasma samples from seven iTTP patients (Aix Marseille Univ, Marseille, France) and one healthy donor (HD) (KU Leuven Campus Kulak Kortrijk, Kortrijk, Belgium) were collected and stored at -80 °C until further use. A normal human plasma pool (NHP, plasma from ≥ 20 healthy donors) was prepared at KU Leuven Campus Kulak, Kortrijk and stored at -80 °C until further use. The study protocol was approved by the local Ethical Committees (for Aix Marseille Univ: Projet National de Recherche Clinique 2007: #2007/23; for KU Leuven Campus Kulak Kortrijk: project 260220). Informed consent was obtained from each patient according to the Declaration of Helsinki.

Preparation of ADAMTS13-depleted plasma. Tosylactivated magnetic beads (2.5 mg) were functionalized with 50 µg of mouse monoclonal anti-human ADAMTS13 antibody 17C7 in PBS as previously described[29,30]. One milligram of the functionalized magnetic beads was transferred to an Eppendorf tube and washed twice with HEPES buffer. With help of a magnet, all supernatant was removed and 500 µL of HD plasma was added. The suspension was rotated for 1 h at room temperature to allow the binding of plasma ADAMTS13 to the monoclonal antibody 17C7. Next, the Eppendorf tube was placed on a magnet and the plasma was transferred into a new tube containing 1 mg of functionalized beads. This process was repeated twice. Plasma was collected into a new Eppendorf tube and stored at -80 °C until further use. The successful depletion of ADAMTS13 was confirmed by ELISA as previously described[27,31] with minor modifications (Figure S1). Colorimetric development was performed with TMB substrate solution. The reaction was stopped with 2 M H_2SO_4, and the absorbance was measured at 450 nm.

FO-SPR platform and functionalization of the FO probes. Experiments were performed at 37 °C on an FO-SPR platform (White FOx 1.0) commercialized by FOx Biosystems (Diepenbeek, Belgium). A detailed description of the FO-SPR platform and the preparation of the gold-coated FO probes can be found in Lu et al. (2016). The gold-coated FO probes were functionalized with a 0.2 mM solution of NTA-SAM upon overnight incubation at 4 °C. Before use, NTA functionalized FO probes were rinsed with ethanol and transferred to HEPES buffer. Depending on the experimental set-up, FO probes were chelated with Co(II) or Ni(II) by immersing the FO probes in 40 mM $CoCl_2$ or 40 mM $NiSO_4$ (dissolved in MQ water) for 10 min. Next, the FO probes were washed by immersing the probes in HEPES buffer for 5 min. rADAMTS13-His_6 (diluted in HEPES buffer) was then immobilized on the NTA-Co(II) or NTA-Ni(II) FO probes for 20 min while shaking at 300 rpm. To study the optimal concentration for antigen immobilization, NTA-Co(II) FO probes were immersed in rADAMTS13-His_6 solutions of different concentrations (2.5, 5, 7.5, 10, 12.5 and 15 µg/mL). For further experiments, 10 µg/mL rADAMTS13-His_6 was used. Afterwards, FO probes with NTA-Co(II)-rADAMTS13-His_6 complex were immersed for 30 min in 10 mM H_2O_2 (diluted in Tris-NaCl buffer) to oxidize Co(II) to Co(III). In the case of NTA-Ni(II)-rADAMTS13-His_6 complex this step was not performed.

FO-SPR assay for anti-ADAMTS13 autoantibody detection in buffer and plasma. To detect anti-ADAMTS13 autoantibodies in buffer or plasma, functionalized FO probes were first blocked using SuperBlock™ blocking buffer for 12 min after which the FO probes were immersed in Tris-NaCl buffer for 6 min. The FO probes were then immersed in the samples for 20 min while shaking at 150 rpm. The samples were prepared as follows: (i) To evaluate the assay specificity, 50 ng/mL of anti-ADAMTS13 autoantibody II-1 and 1 µg/mL non-specific IgG were diluted in Tris-NaCl buffer. (ii) To build a calibration curve, a serial dilution of anti-ADAMTS13 autoantibody II-1 was prepared in 80-fold diluted ADAMTS13-depleted plasma in Tris-NaCl buffer. The final concentration of anti-ADAMTS13 autoantibody II-1 ranged from 0 to 100 ng/mL (0, 1.56, 3.13, 6.25, 12.5, 25, 50, 100 ng/mL). (iii) To measure the presence of autoantibodies in plasma samples of iTTP patients, samples were thawed for 5 min at 37 °C and 80-fold diluted in Tris-NaCl buffer. After binding of the autoantibodies, the FO probes were immersed once again in Tris-NaCl buffer for 6 min followed by another 6 min incubation step in Tris-NaCl buffer with 0.5 % BSA (w/v). To enhance the SPR signal, FO probes were immersed in an anti-human IgG-AuNPs solution (preparation described below) for 20 min. A typical sensorgram of the SPR immunoassay for anti-ADAMTS13 autoantibody is shown in Figure 1B.

Surface functionalization of AuNPs with anti-human IgG antibodies. The AuNPs were conjugated with goat anti-human IgG antibodies via physical adsorption as described previously[13]. Briefly, the pH of the AuNP solution was adjusted

to 9.2 using 0.2 mM of a sodium carbonate solution (pH 11). Then, goat anti-human IgG antibodies were added to 800 µL of the AuNPs solution at a final concentration of 5 µg/mL. The solution was incubated for 20 min at room temperature under continuous rotation. Next, 560 µL of Tris-NaCl buffer with 0.5 % BSA (w/v) was added to block the remaining free active sites on the functionalized AuNPs. The solution was incubated for 1 h at room temperature under continuous rotation and then centrifuged for 30 min at 7000 rpm. The supernatant was carefully removed, and the pellet was resuspended in Tris-NaCl buffer with 0.5 % BSA (w/v). Finally, the optical density (OD) of the anti-human IgG-AuNPs was measured using a spectrophotometer (SpectraMax iD3, Molecular devices, San Jose, California, USA) and the OD value was adjusted to 0.5 using the Tris-NaCl buffer with 0.5 % BSA (w/v)

ELISA for measurement of anti-ADAMTS13 autoantibodies. Anti-ADAMTS13 autoantibodies in plasma of iTTP patients were measured using our in-house developed ELISA. In brief, 15 nM of rADAMTS13-His_6 (diluted in PBS with 0.3 % milk (w/v)) was added to the wells of a Pierce™ nickel-coated plate for 1.5 h at room temperature under constant shaking (150 rpm). Next, the plates were washed three times with PBS containing 0.1 % Tween 20 (v/v). To build a calibration curve, a serial dilution of anti-ADAMTS13 autoantibody II-1 was prepared in PBS with 0.3 % milk (w/v). The starting concentration of anti-ADAMTS13 autoantibody II-1 was 25 ng/mL which was then further diluted to 1:2. Before measuring the presence of autoantibodies in plasma samples of iTTP patients, the samples were thawn for 5 min at 37 °C and, starting from dilution of 1/80, a ½ dilution series was prepared. Samples were then added to the rADAMTS13-His_6 coated wells and incubated for 1 h at room temperature. Bound autoantibodies were detected using goat anti-human IgG antibodies (1:10 000 in PBS with 0.3 % milk (w/v)) followed by addition of rabbit anti-goat IgG HRP labelled antibodies (1:10 000 in PBS with 0.3 % milk (w/v)). Colorimetric development was performed with OPD and H_2O_2. The reaction was stopped with 4 M H_2SO_4, and the absorbance was measured at 492 nm.

Data analysis. The SPR signals (in nm) were recorded with FOx software (FOx Biosystems) at a 2 Hz sampling rate. The data was processed using Graphpad Prism v5.03 software (GraphPad Software, San Diego, CA, USA). A non-linear regression (one-site binding) was applied for curve fitting (eq. (1)) where x represents the autoantibody concentration, y the final SPR shift and A and B the fitting curve parameters[13].

(1) y=(x*A)/(x+B)

To calculate the limit of detection (LoD), eq. (2) was applied where $y(0)$ is the mean SPR shift of the depleted plasma and σ is the standard deviation on this signal [13].

(2) LoD=((y(0)+3σ)*B)/(A-(y(0)+3σ))

The coefficient of variation (CV) was applied to evaluate the dispersion of the dataset and was calculated by dividing the standard deviation (σ) by the mean ($\bar{x}$). To compare different groups, the data was statistically analyzed with one-way ANOVA with Tukey's multiple comparison test (α-level of 0.05). Pearson correlation was used to determine the correlation between two groups.

RESULTS AND DISCUSSION

FO-SPR immunoassay for the detection of anti-ADAMTS13 autoantibodies. To detect anti-ADAMTS13 autoantibodies, rADAMTS13-his_6 was first immobilized on the FO-SPR surface based on the Co(III)-NTA strategy [23] as represented in Figure 1A. In the following step, the anti-ADAMTS13 autoantibodies were then bound to the immobilized antigen and detected by AuNPs pre-functionalized with anti-human IgG antibody as a signal enhancement strategy (Figure 1B). In the following sections we discuss the optimization and characterization of this bioassay in more detail.

Optimization of rADAMTS13-His_6 immobilization on the FO probe surface. The efficiency of rADAMTS13-His_6 immobilization on the sensor surface depends on the

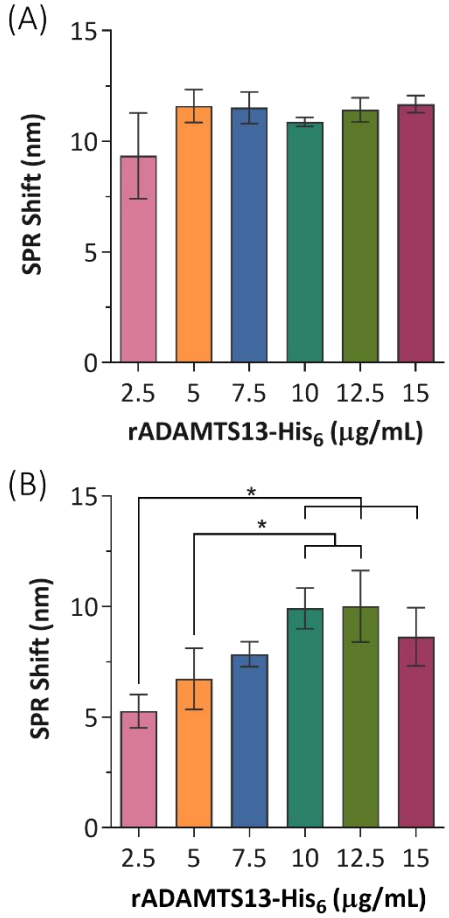

Figure 2. Optimizing the concentration of rADAMTS13-His_6 in the FO-SPR immunoassay A) Immobilization SPR shifts obtained at the end of the rADAMTS13-His_6 immobilization step (step 2, Figure 1) when adding different concentrations of rADAMTS13-His_6 (in HEPES buffer). Error bars represent one standard deviation (n=3). B) Final SPR shifts at the end of the anti-human IgG-AuNPs amplification step (step 6, Figure 1) when using different rADAMTS13-His_6 concentrations in the immobilization step. A concentration of 50 ng/mL anti-ADAMTS13 autoantibody II-1 was used in each experiment (step 5, Figure 1). Error bars represent one standard deviation (n=3). Significant differences are indicated with (*) ($p < 0.05$).

rADAMTS13-His_6 concentration. Hereto we first evaluated the magnitude of the obtained SPR shift as function of the rADAMTS13-His_6 concentration (2.5, 5, 7.5, 10, 12.5 and 15 µg/mL diluted in HEPES buffer). The SPR shift was evaluated at the end of two different steps – the end of the rADAMTS13-His_6 immobilization step (immobilization SPR shift, step 2) and the end of the anti-human IgG-AuNPs signal amplification step (final SPR shift, step 6). The immobilization SPR shifts and the final SPR shifts are represented in Figure 2A and 2B, respectively. Using concentrations between 2.5 and 15 µg/mL rADAMTS13-His_6 did not result in significantly different immobilization SPR shifts (Figure 2A). However, when adding 50 ng/mL of anti-ADAMTS13 autoantibody II-1 to the different rADAMTS13-His_6 concentrations, differences in final SPR shifts were observed (Figure 2B). The highest SPR signal was observed when rADAMTS13-His_6 concentrations of 10 and 12.5 µg/mL were used. Hence, for all future experiments, we worked with 10 µg/mL rADAMTS13-His_6 (Figure 2B).

Specificity of the FO-SPR immunoassay. The specificity of the FO-SPR immunoassay was studied by testing several negative controls. For these controls each time one reagent from the FO-SPR immunoassay was omitted or changed in different experiments and final SPR shifts (step 6, Figure 1) were reported for every experiment (Figure S2): absence of rADAMTS13-His_6 (Figure S2, column A), absence of the anti-ADAMTS13 autoantibody II-1 (Figure S2, column B) and addition of a non-specific IgG instead of anti-ADAMTS13 autoantibody II-1 (Figure S2, column C). As a positive control, rADAMTS13-His_6 and 50 ng/mL the anti-ADAMTS13 autoantibody II-1 were used (Figure S2, column D). The data in Figure S2 shows that the FO-SPR immunoassay was specific as all negative controls were not significantly different from zero.

Biosensor performance as function of the Co(III) versus Ni(II)-NTA coupling strategy. In our recently published report, we described the application of Co(III)-NTA chemistry for oriented patterning of bioreceptors on FO-SPR biosensors in complex matrices using a model system[26]. The application of Co(III)-NTA chemistry for binding of autoantibodies to the bioreceptor in clinical samples has not been explored yet. We hypothesized that rADAMTS13-His_6 immobilization on a Co(III)-NTA surface would result in an increased surface stability of rADAMTS13-His_6 when working with plasma samples compared to immobilization on a Ni(II)-NTA surface. An increased surface stability of rADAMTS13-His_6 on a Co(III)-NTA surface would then result in a higher and more stable final SPR shift when detecting anti-ADAMTS13 autoantibodies present in plasma of an iTTP patient compared to the use of an Ni(II)-NTA surface.

We therefore performed the FO-SPR immunoassay using a 40-fold diluted plasma sample of an iTTP patient, known to have a high titer of anti-ADAMTS13 autoantibodies[32], and compared the final SPR shift when rADAMTS13-His_6 was immobilized via the Co(III)-NTA strategy or via the Ni(II)-NTA strategy (Figure 3). A significantly higher final SPR shift (step 6, Figure 1) was observed for the Co(III)-NTA strategy compared to Ni(II)-NTA strategy (Figure 3A, left two columns). As a control, we performed the same experiments in a plasma-free environment, using anti-ADAMTS13 autoantibody II-1 in buffer and also here compared the final SPR shift (step 6, Figure 1) when rADAMTS13-His_6 was immobilized via the Co(III)-NTA strategy or via the Ni(II)-NTA strategy. No significant difference in the final SPR shifts between the two conditions was observed (Figure 3A, right two columns).

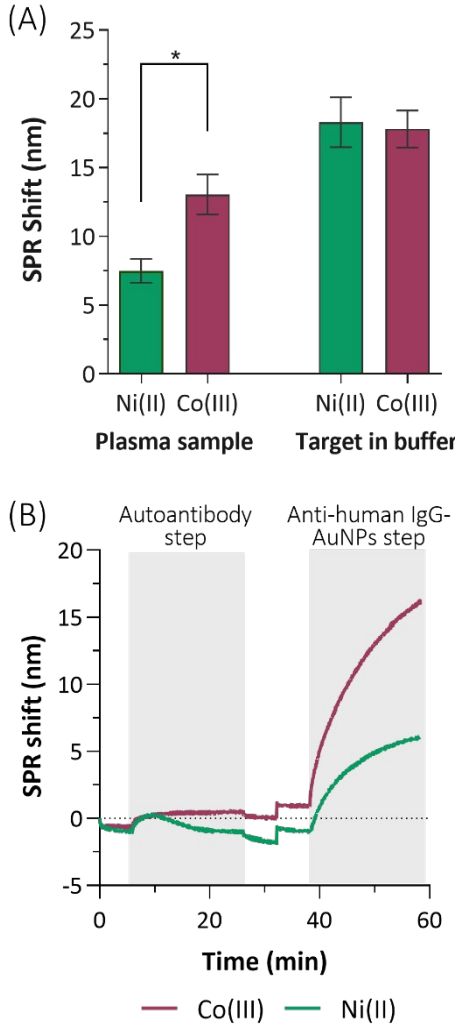

Figure 3. Influence of the rADAMTS13-His_6-coupling strategy (Ni(II)-NTA versus Co(III)-NTA) on the FO-SPR immunoassay. A) Stability of the rADAMTS13-His_6-coupling in buffer or plasma as function of the coupling strategy. Final SPR shift measured after the IgG-AuNPs amplification step with either 40-fold diluted plasma sample of an iTTP patient known to have a high titer of anti-ADAMTS13 antibodies (plasma sample) or 50 ng/mL anti-ADAMTS13 autoantibody II-1 (target in buffer). Error bars represent one standard deviation (n=3). Significant differences are represented with (*) ($p < 0.05$). B) SPR sensorgram recorded for the Co(III) and Ni(II) surface, during incubation with a 40-fold diluted plasma sample containing anti-ADAMTS13 antibodies (left shaded zone) and during the amplification step with anti-human IgG-AuNPs (right shaded zone).

Similar experimental design was performed to compare Co(III) to Co(II) strategy and we observed that the charge of the chelating ion plays a critical role in the stability of the complex (data not shown). Hence, the higher final SPR shift observed using the Co(III)-NTA strategy compared to the Ni(II)-NTA and Co(II)-NTA strategy, when working in a plasma environment, might be explained by the increased stability of the rADAMTS13His_6-NTA complexes formed with trivalent ions as Co(III) compared to divalent ions as Ni(II) and Co(II). Indeed, during the exposure of the plasma sample to the Ni(II)-

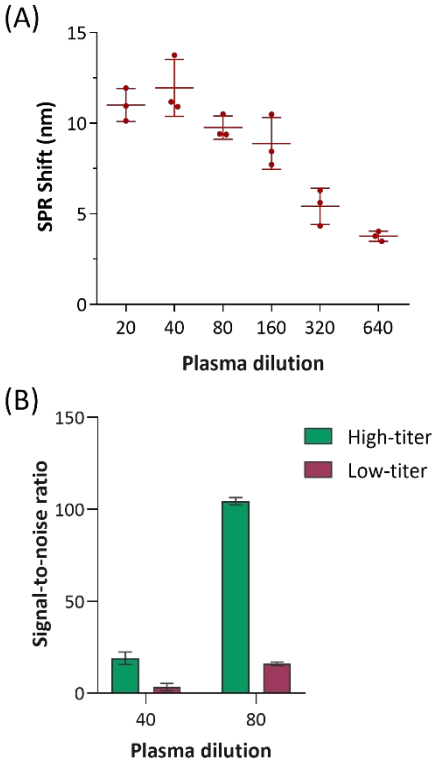

Figure 4. Summary of final SPR shifts obtained from testing different dilutions of iTTP plasma samples. A) Serial dilution of a plasma sample with high anti-ADAMTS13 autoantibody titers. Final SPR shifts measured after the anti-human IgG-AuNPs amplification step in 20-, 40-, 80-, 160-, 320-, 640-fold diluted plasma samples. Error bars represent the standard deviation (n=3) B) Signal-to-noise ratio (SNR) of two iTTP patient plasma samples with high and low anti-ADAMTS13 autoantibody titers. To calculate the SNR, final SPR shifts obtained for each sample were divided by final SPR shifts obtained for NHP sample with 40- and 80-fold dilution. Error bars represent the standard deviation (n=4).

NTA-rADAMTS13-His_6 FO-SPR probe (step 5, Figure 1), a decrease in SPR shift was observed which was not observed when the Co(III)-NTA-rADAMTS13-His_6 FO-SPR probe was used (Figure 3B). This decrease is very likely caused by the dissociation of rADAMTS13-His_6 from the Ni(II)-NTA surface under influence of the metal-binding proteins present in plasma[20].

FO-SPR immunoassay: analyzing different dilutions of iTTP plasma samples. For the abovementioned experiment, we used a 40-fold dilution of an ITTP plasma sample. However, it is important to study the dilution factor of plasma that gives a good signal-to-noise ratio (SNR) in our FO-SPR immunoassay. Therefore, two iTTP plasma samples were selected: one sample known to have a high and one with a low anti-ADAMTS13 autoantibody titer (high >0.5 µg/mL II-1 equivalents; low < 0.1 µg/mL II-1 equivalents). As a negative control, NHP was used.

Initially, a dilution series of an iTTP plasma sample with high anti-ADAMTS13 autoantibody titers was measured in the FO-SPR immunoassay (Figure 4A). A serial dilution was performed ranging from 20-, 40-, 80-, 160-, 320- and 640-fold dilution. As demonstrated in Figure 4A, the three lowest dilutions (20-, 40- and 80-fold dilution) demonstrated the highest final SPR shift for detection of anti-ADAMTS13 autoantibodies. Since the final SPR shifts with the 40- and 80-times diluted plasma samples gave high final SPR shifts and lower amounts of plasma were needed than when using the 20 diluted plasma samples, we used these two conditions to further look into the SNR. For this purpose, a plasma sample from an iTTP patient with low anti-ADAMTS13 autoantibody titers and one NHP sample were measured under 40- and 80-fold dilution. Figure 4B shows that the SNR was higher when applying an 80-fold plasma dilution and for this reason we opted to use the 80-fold plasma dilution for detecting anti-ADAMTS13 autoantibodies in plasma samples.

Calibration curve and LoD of the assay. Next, a calibration curve was made where anti-ADAMTS13 autoantibody II-1 was diluted in 80-fold diluted ADAMTS13-depleted plasma (Figure 5A). To evaluate the repeatability of the assay, the calibration curve was performed in triplicate, with each repetition being performed on a different day on two different FO-SPR platforms. The SPR shifts are plotted as a function of the anti-ADAMTS13 autoantibody II-1 concentration (Figure 5A). The corresponding coefficients of variation (CV) are given in Table S1. Each point of the calibration curve displayed an inter-assay CV below 15 % and the average inter-assay CV was 7.1 %. The LoD was calculated as described in Section 2.3 using 80-fold diluted ADAMTS13-depleted plasma and was equal to 0.24 ng/mL II-1 equivalents. This result is comparable with the LoD of our in-house ELISA (LoD < 1 ng/mL). The detection of 0.24 ng/mL II-1 equivalents in 80-fold plasma translates to a 19.2 ng/mL II-1 equivalents detection limit in undiluted plasma showing the high sensitivity of the presented FO-SPR immunoassay. The final SPR shift of the calibration curve with anti-ADAMTS13 autoantibody II-1 diluted in the depleted plasma was also compared with same antibody dilution series performed in buffer (Figure S3). Comparable final SPR shifts were obtained demonstrating the stability of the assay when adding plasma.

Validation of the biosensor performance with ELISA using plasma samples of iTTP patients. Finally, we validated the developed FO-SPR immunoassay using seven plasma samples from iTTP patients known to have anti-ADAMTS13 autoantibodies. For the FO-SPR immunoassay, all plasma samples were 80-fold diluted and the concentrations calculated using the calibration curve established using anti-ADAMTS13 autoantibody II-1 spiked in 80-fold diluted ADAMTS13-depleted plasma (Figure 5A). The experiments were performed in triplicate, on three different days, and then compared with those obtained from the in-house developed ELISA. The in-house developed ELISA consisted of a similar setup as the FO-SPR bioassay (capturing rADAMTS13-His_6 via NTA and detecting bound anti-ADAMTS13 autoantibodies using the same anti-human IgG), as we have recently shown that anti-ADAMTS13 autoantibody titers in iTTP patients is influenced by the way ADAMTS13 is coated and by the type of detection antibody used (Dekimpe et al. unpublished).

As represented in Figure 5B, the concentrations measured by the developed FO-SPR immunoassay were correlated with those measured via the in-house developed ELISA and a significant Pearson correlation of 0.973 was obtained. In addition, advantages of the FO-SPR bioassay over ELISA are a short assay time and the potential for full automation of the assay (plasma samples are simply added to the FOx device and

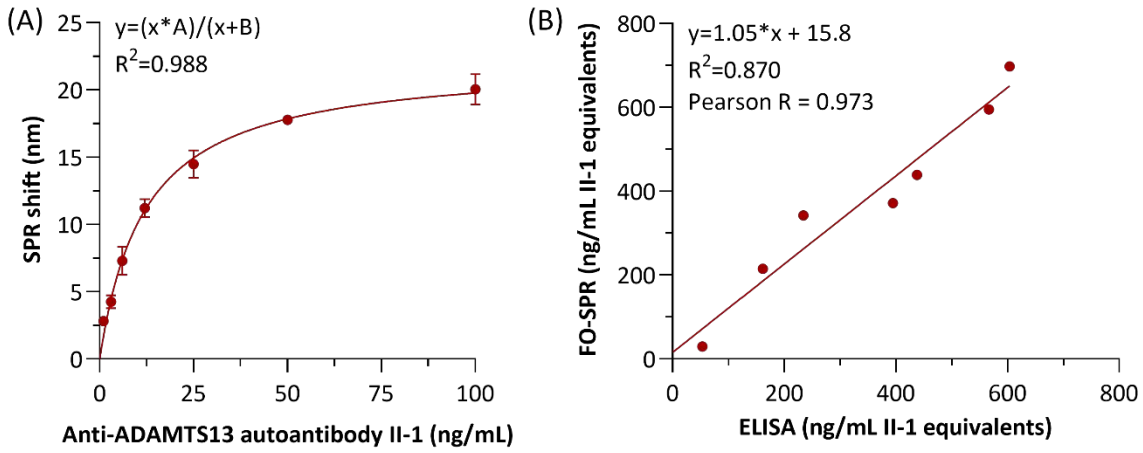

Figure 5. FO-SPR immunoassay to quantify anti-ADAMTS13 autoantibodies in patient plasma. A) Calibration curve obtained from a two-fold dilution series of anti-ADAMTS13 autoantibody II-1 in 80-fold diluted ADAMTS13 depleted plasma. A nonlinear regression (one-site binding) was applied to fit the entire concentration range. Fitting parameters are A=22.16 nm (95% CI=21.09 to 23.31) and B=12.06 ng/mL (95% CI=10.26 to 14.18). Error bars represent one standard deviation (n=3). B) Comparison of the FO-SPR assay and the ELISA to measure anti-ADAMTS13 autoantibodies in plasma samples of seven iTTP patients. The Pearson correlation was 0.973 with a p-value of 0.0002. A linear regression was applied to fit the data. Fitting parameters are slope=1.05 (95% CI=0.8571 to 1.248) and Y-intercept=15.77 (95% CI=-62.26 to 93.80). Experiments were performed in triplicate for both ELISA and the FO-SPR platform.

dipping of the FO-SPR in the plasma and addition of the reagents can be fully automated). The total FO-SPR assay time of 2.5 h as reported here is shorter than the total assay time of ~4-5 h and can even be reduced to 5 mins when the assay runs fully automated. These results show the potential of optical sensors as FO-SPR for automated, reliable and fast detection of autoantibodies in plasma samples. The reduction of detection time to up to 5 mins and multiplexing are some of added features of the FO-SPR method that can be further explored[13,26].

CONCLUSIONS

One of the biggest challenges in modern diagnostics is the timely diagnosis of diseases which makes biosensors an invaluable tool for the simple and rapid detection of a multitude of analytes. However, complex matrices often pose a problem for achieving the needed sensitivities. Therefore, the development of biosensors with robust surface chemistries to enable sample detection in complex matrices becomes crucial.

In this study we described for the first time the development of a fast and easy-to-use FO-SPR immunoassay for the detection and quantification of anti-ADAMTS13 autoantibodies in plasma. To achieve this, rADAMTS13-His_6 was immobilized on an FO probe by His_6-tag interaction with NTA-SAM using Co(III)-NTA strategy. After blocking, FO probes were exposed to autoantibodies and the signal was amplified using anti-human IgG-AuNPs. The performance was improved by optimizing the immobilization of rADAMTS13-His_6 and the reliability of the developed biosensor was studied by measuring different quality controls. At a concentration of 10 µg/mL of rADAMTS13-His_6, the results demonstrated high specificity of the immunoassay. The stability of this method was also confirmed by challenging Co(III)- and Ni(II)-NTA surface with a plasma sample with high anti-ADAMTS13 autoantibody titers, observing a significantly higher SPR shift in probes with Co(III)-NTA compared to Ni(II)-NTA. For analysis of anti-ADAMTS13 autoantibodies in plasma samples, a calibration curve was built using dilutions of the anti-ADAMTS13 antibody II-1 in 80-fold diluted ADAMTS13-depleted plasma. The FO SPR immunoassay demonstrated a high sensitivity with an LoD of 0.24 ng/mL II-1 equivalents. Finally, we validated the developed FO-SPR immunoassay using seven plasma samples from iTTP patients and compared the results with the in-house developed ELISA. An excellent correlation of 0.973 between both methods was observed. The results confirmed the reliability of the FO-SPR immunoassay and its suitability for clinical diagnostics of iTTP.

iTTP is only one of many life-threatening autoimmune diseases that requires simple and automated analytical tools to support clinical decisions. With our biosensor-based assay, we aim to improve diagnosis and prognosis of immune-related disorders as rheumatoid arthritis and type 1 diabetes mellitus by allowing fast and simple detection of antigen-specific antibodies.

ASSOCIATED CONTENT

Supporting Information

The Supporting Information is available free of charge on the ACS Publications website.

Quantification of human ADAMTS13 in a depleted healthy donor (HD) plasma sample; Specificity of the FO-SPR immunoassay; Summary of final SPR shifts and respective inter-assay CV's calculated for each point in the calibration curve; Comparison of the SPR signals in the measurement of anti-ADAMTS13 autoantibody II-1 in ADAMTS13-depleted plasma and in buffer (PDF)

AUTHOR INFORMATION

Corresponding Author

*Last authors and corresponding authors: Karen Vanhoorelbeke (Email: karen.vanhoorelbeke@kuleuven.be, ORCID: 0000-0003-2288-8277) and Jeroen Lammertyn (Email: jeroen.lammertyn@kuleuven.be, ORCID: 0000-0001-8143-6794)

Author Contributions

S.H. designed and optimized the protocols, performed the experiments, analyzed data and wrote the manuscript; J.Q. and C.D. were involved in discussions and provided technical help in the lab; Q.B. and A.V. performed the experiments; E.T. and G.K. provided clinical samples; F.D interpreted data and critically reviewed the manuscript; N.G supervised, conceived the study, analyzed data and critically reviewed the manuscript; J.L. and K.V. supervised, designed the experiments, analyzed data, wrote and reviewed the manuscript. All authors discussed the results and provided their critical feedback on the manuscript. All authors have given approval to the final version of the manuscript.

Conflict of Interest Disclosure:
"J.L. is member of the board of directors of FOx Biosystems, a spin-off of the KU Leuven".

ACKNOWLEDGMENT

This work was supported by the "Fonds voor Wetenschappelijk Onderzoek - Toegepast Biomedisch onderzoek met een primair Maatschappelijke finaliteit" (FWO-TBM) (T002918N) awarded to K. Vanhoorelbeke. S. Horta scholarship was funded by the European Union's Horizon 2020 research and innovation programme under the Marie Skłodowska-Curie grant agreement No 675412 (H2020-MSCA-ITN-ND4ID). We would like to thank Jan Voorberg (Sanquin Research and Landsteiner Laboratory, University of Amsterdam, the Netherlands) for providing the anti-ADAMTS13 autoantibody II-1. Table of contents (TOC) created with Biorender.com.

REFERENCES

(1) Zhang, X.; Zambrano, A.; Lin, Z. T.; Xing, Y.; Rippy, J.; Wu, T. Immunosensors for Biomarker Detection in Autoimmune Diseases. *Arch. Immunol. Ther. Exp. (Warsz).* **2017**, *65* (2), 111–121.

(2) Ludwig, R. J.; Vanhoorelbeke, K.; Leypoldt, F.; Kaya, Z.; Bieber, K.; McLachlan, S. M.; Komorowski, L.; Luo, J.; Cabral-Marques, O.; Hammers, C. M.; Lindstrom, J. M.; Lamprecht, P.; Fischer, A.; Riemekasten, G.; Tersteeg, C.; Sondermann, P.; Rapoport, B.; Wandinger, K. P.; Probst, C.; Beidaq, A. El; Schmidt, E.; Verkman, A.; Manz, R. A.; Nimmerjahn, F. Mechanisms of Autoantibody-Induced Pathology. *Front. Immunol.* **2017**, *8* (603), 1–42.

(3) Lerner, A.; Jeremias, P.; Matthias, T. The World Incidence and Prevalence of Autoimmune Diseases Is Increasing. *Int. J. Celiac Dis.* **2016**, *3* (4), 151–155.

(4) Kremer Hovinga, J. A.; Coppo, P.; Lämmle, B.; Moake, J. L.; Miyata, T.; Vanhoorelbeke, K. Thrombotic Thrombocytopenic Purpura. *Nat. Rev. Dis. Prim.* **2017**, *3* (1), 17020.

(5) Joly, B. S.; Coppo, P.; Veyradier, A. Thrombotic Thrombocytopenic Purpura. *Blood* **2017**, *129* (21), 2836–2848.

(6) Tersteeg, C.; Verhenne, S.; Roose, E.; Schelpe, A. S.; Deckmyn, H.; De Meyer, S. F.; Vanhoorelbeke, K. ADAMTS13 and Anti-ADAMTS13 Autoantibodies in Thrombotic Thrombocytopenic Purpura-Current Perspectives and New Treatment Strategies. *Expert Rev. Hematol.* **2016**, *9* (2), 209–221.

(7) Alwan, F.; Vendramin, C.; Vanhoorelbeke, K.; Langley, K.; McDonald, V.; Austin, S.; Clark, A.; Lester, W.; Gooding, R.; Biss, T.; Dutt, T.; Cooper, N.; Chapman, O.; Cranfield, T.; Douglas, K.; Watson, H. G.; Van Veen, J. J.; Sibson, K.; Thomas, W.; Manson, L.; Hill, Q. A.; Benjamin, S.; Ellis, D.; Westwood, J. P.; Thomas, M.; Scully, M. Presenting ADAMTS13 Antibody and Antigen Levels Predict Prognosis in Immune-Mediated Thrombotic Thrombocytopenic Purpura. *Blood* **2017**, *130* (4), 466–471.

(8) Peyvandi, F.; Palla, R.; Lotta, L. A.; Mackie, I.; Scully, M. A.; Machin, S. J. ADAMTS-13 Assays in Thrombotic Thrombocytopenic Purpura. *J. Thromb. Haemost.* **2010**, *8* (4), 631–640.

(9) Scheiflinger, F.; Knöbl, P.; Trattner, B.; Plaimauer, B.; Mohr, G.; Dockal, M.; Dorner, F.; Rieger, M. Nonneutralizing IgM and IgG Antibodies to von Willebrand Factor-Cleaving Protease (ADAMTS-13) in a Patient with Thrombotic Thrombocytopenic Purpura. *Blood* **2003**, *102* (9), 3241–3243.

(10) Thévenot, D. R.; Toth, K.; Durst, R. A.; Wilson, G. Electrochemical Biosensors: Recommended Definitions and Classification. *Electroanal. Chem.* **1999**, *71* (12), 2333–2348.

(11) Qu, J.-H.; Dillen, A.; Saeys, W.; Lammertyn, J.; Spasic, D. Advancements in SPR Biosensing Technology: An Overview of Recent Trends in Smart Layers Design, Multiplexing Concepts, Continuous Monitoring and in Vivo Sensing. *Anal. Chim. Acta* **2020**, *1104*, 10–27.

(12) Lu, J.; Spasic, D.; Delport, F.; Van Stappen, T.; Detrez, I.; Daems, D.; Vermeire, S.; Gils, A.; Lammertyn, J. Immunoassay for Detection of Infliximab in Whole Blood Using a Fiber-Optic Surface Plasmon Resonance Biosensor. *Anal. Chem.* **2017**, *89* (6), 3664–3671.

(13) Lu, J.; Van Stappen, T.; Spasic, D.; Delport, F.; Vermeire, S.; Gils, A.; Lammertyn, J. Fiber Optic-SPR Platform for Fast and Sensitive Infliximab Detection in Serum of Inflammatory Bowel Disease Patients. *Biosens. Bioelectron.* **2016**, *79*, 173–179.

(14) Bian, S.; Lu, J.; Delport, F.; Vermeire, S.; Spasic, D.; Lammertyn, J.; Gils, A. Development and Validation of an Optical Biosensor for Rapid Monitoring of Adalimumab in Serum of Patients with Crohn's Disease. *Drug Test. Anal.* **2018**, *10* (3), 592–596.

(15) Kim, J.; Kim, S. J.; Nguyen, T. T.; Lee, R.; Li, T.; Yun, C.; Ham, Y.; An, S. S. A.; Ju, H. Label-Free Quantitative Immunoassay of Fibrinogen in Alzheimer Disease Patient Plasma Using Fiber Optical Surface Plasmon Resonance. *J. Electron. Mater.* **2016**, *45* (5), 2354–2360.

(16) Shen, M.; Rusling, J. F.; Dixit, C. K. Site-Selective Orientated Immobilization of Antibodies and Conjugates for Immunodiagnostics Development. *Methods* **2017**, *116*, 95–111.

(17) Hochuli, E.; Bannwarth, W.; Döbeli, H.; Gentz, R.; Stüber, D. Genetic Approach to Facilitate Purification of Recombinant Proteins with a Novel Metal Chelate Adsorbent. *Bio/Technology* **1988**, *6* (11), 1321–1325.

(18) Ueda, E. K. M.; Gout, P. W.; Morganti, L. Current and Prospective Applications of Metal Ion-Protein Binding. *J. Chromatogr. A* **2003**, *988* (1), 1–23.

(19) Mourão, C. A.; Carmignotto, G. P.; Bueno, S. M. A. Separation of Human IgG Fragments Using Copper, Nickel, Zinc, and Cobalt Chelated to CM-Asp-Agarose by Positive and Negative Chromatography. *J. Chromatogr. B Anal. Technol. Biomed. Life Sci.* **2016**, *1017–1018*, 163–173.

(20) Wang, F.; Chmil, C.; Pierce, F.; Ganapathy, K.; Gump, B. B.; MacKenzie, J. A.; Metchref, Y.; Bendinskas, K. Immobilized Metal Affinity Chromatography and Human Serum Proteomics. *J. Chromatogr. B Anal. Technol. Biomed. Life Sci.* **2013**, *934*, 26–33.

(21) Wang, X.; Liu, Q.; Tan, X.; Liu, L.; Zhou, F. Covalent Affixation of Histidine-Tagged Proteins Tethered onto Ni-Nitrilotriacetic Acid Sensors for Enhanced Surface Plasmon Resonance Detection of Small Molecule Drugs and Kinetic Studies of Antibody/Antigen Interactions. *Analyst* **2019**, *144* (2), 587–593.

(22) Ericsson, E. M.; Enander, K.; Bui, L.; Lundström, I.; Konradsson, P.; Liedberg, B. Site-Specific and Covalent Attachment of His-Tagged Proteins by Chelation Assisted Photoimmobilization: A Strategy for Microarraying of Protein Ligands. *Langmuir* **2013**, *29* (37), 11687–11694.

(23) Wegner, S. V.; Spatz, J. P. Cobalt(III) as a Stable and Inert Mediator Ion between NTA and His6-Tagged Proteins. *Angew. Chemie - Int. Ed.* **2013**, *52* (29), 7593–7596.

(24) Wegner, S. V; Schenk, F. C.; Spatz, J. P. Cobalt(III)-Mediated Permanent and Stable Immobilization of Histidine-Tagged Proteins on NTA-Functionalized Surfaces. *Chem. - A Eur. J.* **2016**, *22* (9), 3156–3162.

(25) Auer, S.; Azizi, L.; Faschinger, F.; Blazevic, V.; Vesikari, T.; Gruber, H. J.; Hytönen, V. P. Stable Immobilisation of His-Tagged Proteins on BLI Biosensor Surface Using Cobalt. *Sensors Actuators B Chem.* **2017**, *243*, 104–113.

(26) Qu, J.-H.; Horta, S.; Delport, F.; Sillen, M.; Geukens, N.; Sun, D.-W.; Vanhoorelbeke, K.; Declerck, P.; Lammertyn, J.; Spasic, D. Expanding a Portfolio of (FO-) SPR Surface Chemistries with the Co(III)-NTA Oriented Immobilization of His6-Tagged

Bioreceptors for Applications in Complex Matrices. *ACS Sensors* **2020**.

(27) Roose, E.; Schelpe, A. S.; Joly, B. S.; Peetermans, M.; Verhamme, P.; Voorberg, J.; Greinacher, A.; Deckmyn, H.; De Meyer, S. F.; Coppo, P.; Veyradier, A.; Vanhoorelbeke, K. An Open Conformation of ADAMTS-13 Is a Hallmark of Acute Acquired Thrombotic Thrombocytopenic Purpura. *J. Thromb. Haemost.* **2018**, *16* (2), 378–388.

(28) Pos, W.; Sorvillo, N.; Fijnheer, R.; Feys, H. B.; Kaijen, P. H. P.; Vidarsson, G.; Voorberg, J. Residues Arg568 and Phe592 Contribute to an Antigenic Surface for Anti-Adamts13 Antibodies in the Spacer Domain. *Haematologica* **2011**, *96* (11), 1670–1677.

(29) Schelpe, A. S.; Petri, A.; Roose, E.; Pareyn, I.; Deckmyn, H.; De Meyer, S. F.; Crawley, J. T. B.; Vanhoorelbeke, K. Antibodies That Conformationally Activate ADAMTS13 Allosterically Enhance Metalloprotease Domain Function. *Blood Adv.* **2020**, *4* (6), 1072–1080.

(30) Leirs, K.; Tewari Kumar, P.; Decrop, D.; Pérez-Ruiz, E.; Leblebici, P.; Van Kelst, B.; Compernolle, G.; Meeuws, H.; Van Wesenbeeck, L.; Lagatie, O.; Stuyver, L.; Gils, A.; Lammertyn, J.; Spasic, D. Bioassay Development for Ultrasensitive Detection of Influenza A Nucleoprotein Using Digital ELISA. *Anal. Chem.* **2016**, *88* (17), 8450–8458.

(31) Dekimpe, C.; Roose, E.; Tersteeg, C.; Joly, B. S.; Dewaele, A.; Horta, S.; Pareyn, I.; Vandenbulcke, A.; Deckmyn, H.; Feys, H. B.; Tellier, E.; Kaplanski, G.; Scully, M.; Coppo, P.; De Meyer, S. F.; Veyradier, A.; Vanhoorelbeke, K. Anti-ADAMTS13 Autoantibodies in Immune-mediated Thrombotic Thrombocytopenic Purpura Do Not Hamper ELISA-based Quantification of ADAMTS13 Antigen. *J. Thromb. Haemost.* **2020**, *18* (4), 985–990.

(32) Roose, E.; Schelpe, A.-S.; Tellier, E.; Sinkovits, G.; Joly, B. S.; Dekimpe, C.; Kaplanski, G.; Le Besnerais, M.; Mancini, I.; Falter, D. T.; von Auer, C.; Feys, H. B.; Reti, M.; Rossmann, H.; Vandenbulcke, A.; Pareyn, I.; Voorberg, J.; Greinacher, A.; Benhamou, Y.; Deckmyn, H.; Fijnheer, R. R.; Prohaszka, Z.; Peyvandi, F.; Lämmle, B.; Coppo, P.; De Meyer, S.; Veyradier, A.; Vanhoorelbeke, K. Open ADAMTS13, Induced by Antibodies, Is a Biomarker for Subclinical Immune-Mediated Thrombotic Thrombocytopenic Purpura. *Blood* **2020**, *136* (3), 353–361.

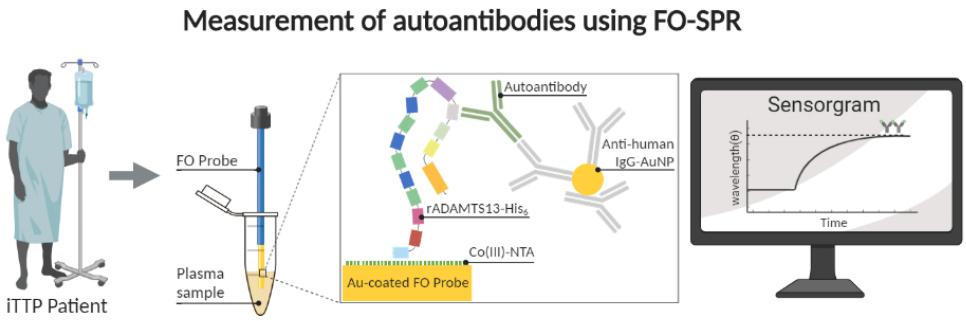

Fiber optic-surface plasmon resonance (FO-SPR) assay for efficient, simple and fast detection of autoantibodies in plasma of patients suffering from the autoimmune disease immune-mediated thrombotic thrombocytopenic purpura (iTTP).